ELSEVIER

Surface Science 493 (2001) 680–686

SURFACE SCIENCE

www.elsevier.com/locate/susc

Two-dimensional plasmon in a surface-state band

Tadaaki Nagao [a,b,c,*], Torsten Hildebrandt [d], Martin Henzler [d], Shuji Hasegawa [a,c]

[a] Department of Physics, Graduate School of Science, The University of Tokyo, 7-3-1 Hongo, Bunkyo-ku, Tokyo 113-0033, Japan
[b] Precursory Research for Embryonic Science and Technology (PRESTO), Japan Science and Technology Corporation (JST), 4-1-8 Honcho, Kawaguchi, Saitama 332-0012, Japan
[c] Core Research for Evolutional Science and Technology (CREST), Japan Science and Technology Corporation (JST), 4-1-8 Honcho, Kawaguchi, Saitama 332-0012, Japan
[d] Institut für Festkörperphysik der Universität Hannover, Appelstraße 2, D-30167 Hannover, Germany

Received 21 September 2000; accepted for publication 13 November 2000

Abstract

By use of electron-energy-loss spectrometer with high-momentum resolution, we have measured a collective electronic excitation in a surface-state band on Si(1 1 1)–$\sqrt{3} \times \sqrt{3}$-Ag. We have clarified that the energy dispersion is isotropic with respect to the azimuthal orientation and shows no dependence on the electron probing depth. The obtained energy dispersion agreed very well with the plasmon dispersion calculated from two-dimensional (2D) nearly free-electron theory. As hallmarked from these observations, we identify the measured loss as a longitudinal intraband 2D plasmon in the surface-state band. © 2001 Published by Elsevier Science B.V.

Keywords: Electron energy loss spectroscopy (EELS); Plasmons; Silicon

1. Introduction

A large number of studies have been done on the *volume* and *surface plasmons* for the bulk and the semi-infinite metallic systems, discussing correlations between plasmons and optical and transport properties, examining dynamic electronic correlation effects [1,2], as well as elucidating nonlocal effects in the dynamical screening at the solid–vacuum interfaces [3–6]. Two-dimensional (2D) plasmon is another different type of plasmon, the charge density distribution of which is restricted in the 2D space and thus shows very different electrodynamical properties compared with those of the above 3D-type plasmons (see Fig. 1). For example, bulk and surface contributions are always inseparable in the properties of the *surface plasmons*. On the contrary, properties of the *2D plasmons* are mainly determined by the properties of the 2D electron system (2DES) itself, especially in the cases of 2DESs supported in (semi-)insulating bulk media. We can take advantage of this characteristic for utilizing the 2D plasmon as a sensitive noncontact probe for 2DES in atomically thin region, such as metallic monolayer or surface-state bands supported on less conductive dielectric media.

By using electron-energy-loss spectroscopy (EELS), we can determine the plasmon energy as a

* Corresponding author. Address: Department of physics, Graduate School of Science, The University of Tokyo, 7-3-1 Hongo, Bunkyo-ku, Tokyo 113-0033, Japan. Tel.: +81-3-5800-3329; fax: +81-3-5800-3329/5841-4209.
E-mail address: nagao@phys.s.u-tokyo.ac.jp (T. Nagao).

0039-6028/01/$ - see front matter © 2001 Published by Elsevier Science B.V.
PII: S0039-6028(01)01282-1

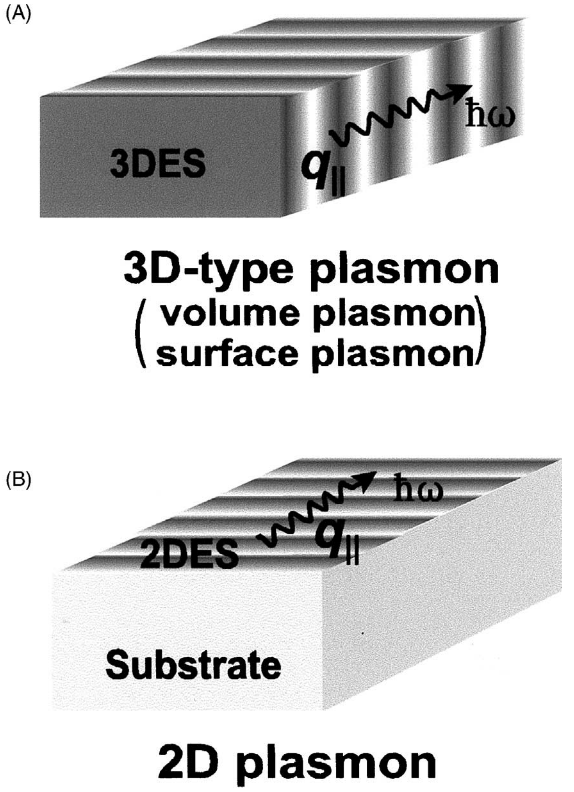

Fig. 1. Schematic illustration explaining the difference between 3D-type plasmons and 2D plasmon.

function of wave number $\boldsymbol{q}_{\|}$ with excellent accessible energy range covering from the far-infrared to ultraviolet regimes. The measurement of energy dispersion curve combined with the theoretical analysis provides us the atomistic information of static and dynamical properties of the 2DES in a great detail. The most suited spectrometer for this purpose is a Henzler-type spectrometer (ELS-LEED; energy-loss-spectroscopy with low-energy electron diffraction) which is possible to operate both as a high-resolution EELS and as a high-resolution low-energy electron diffraction (HRLEED) [7,8]. The improved momentum resolution in 10^{-3} Å^{-1} regime enables us to measure the fine structure by 2D plasmon that steeply disperses and damps in a very small angular window just around the intense Bragg peaks.

In the present paper, we report on the direct measurement of the energy dispersion of a 2D plasmon found in a metallic surface-state band on the Si(1 1 1)–$\sqrt{3} \times \sqrt{3}$-Ag surface. We have clarified the isotropic energy dispersion with respect to the azimuthal orientation as well as no dependence of the energy dispersion on the electron probing depth. We have also found good agreement with the calculated dispersion from 2D nearly free-electron (NFE) theory, and clarified the quantitative agreement with the static electronic properties previously measured by photoelectron spectroscopy (PES).

2. Experimental

The experiment was performed in ultrahigh vacuum with 6×10^{-11} Torr base pressure. The $\sqrt{3} \times \sqrt{3}$-Ag surface was prepared by depositing precisely one monolayer (1 ML) of Ag onto a clean Si(1 1 1)-7 × 7 surface held at around 800 K while keeping the pressure below 1×10^{-9} Torr, and then cooled down to 90 K for EELS measurements. The domain size of the $\sqrt{3} \times \sqrt{3}$ structure was evaluated by ELS-LEED operated in spot profile analysis low-energy electron diffraction (SPA-LEED) mode and was confirmed to be larger than 600 Å (which corresponds to 0.01 Å^{-1} in reciprocal space) so that the plasmon can propagate freely in the long-wavelength limit without being damped by domain-boundary scattering. The energy resolution of the spectra was 20–30 meV which was mostly limited by the broadening due to multi-plasmon and intraband single particle excitations in the metallic surface-state and also in the surface space-charge layer.

3. Results and discussion

A surface-state band on the Si(1 1 1)–$\sqrt{3} \times \sqrt{3}$-Ag surface is one of the most promising prototype system for investigating 2D plasmons. Electronic band structure as well as atomic structure are well established both theoretically and experimentally [9]. There is a shallow electron pocket centered at the Γ point of the surface Brillouin zone of a nearly parabolic band called S1 state. From this band structure, this system can be regarded as a

2D NFE gas. We already know the carrier density in this electron pocket $N_{2D} = (1.6 \pm 0.3) \times 10^{13}$ cm^{-2} and the effective mass $m^* = (0.29 \pm 0.05)m_e$ (m_e is the free-electron mass), estimated from PES measurements [10].

Fig. 2 shows the LEED patterns as obtained by the ELS-LEED operated in the LEED mode using elastic and inelastic beams. Two panels in the upper left (A) and in the upper right (B) shows the diffraction patterns measured from the clean Si(1 1 1)-7 × 7 and from the Si(1 1 1)–$\sqrt{3} \times \sqrt{3}$-Ag surfaces, respectively, using the elastic beam. The data are displayed in logarithmic scale but show low background attributed to the reduced thermal diffuse scattering because of the sufficient energy filtering of the electron beam. The lower panel (C) shows an inelastic 2D scan obtained from the Si(1 1 1)–$\sqrt{3} \times \sqrt{3}$-Ag surface at a loss energy of 400 meV corresponding to the wave number region shown by a white square in Fig. 2(B). The intensity distribution in (C) exhibits nearly isotropic feature with respect to the azimuthal orientation, which indicates the isotropic nature of the excitation.

Angle-resolved electron-energy-loss spectra taken at 90 K from the Si(1 1 1)–$\sqrt{3} \times \sqrt{3}$-Ag surface are shown in Fig. 3(A) and (B). The left panel (A) shows the dependence on the electron primary energy E_p of the peak positions of the losses for the three fixed values of $\boldsymbol{q}_\parallel$. As shown clearly, the loss peaks do not shift in energy position as a function of E_p, which indicates that the excitation energy does not shift by changing the electron probing depth. The peak positions shift only when the momentum transfer (or wave number) $\boldsymbol{q}_\parallel$ is changed by changing the angles θ_i and θ_s (see inset in Fig. 2). By comparing the results obtained from n-type 15 Ω cm silicon wafer and from p-type 0.05 Ω cm wafer, it was also clarified that the change in the doping type and concentration does not affect the peak positions, either. These facts indicate that the excitation has its origin neither in the surface space-charge layer nor in the bulk, and thus can be unambiguously assigned to the excitation in the topmost surface layer.

Fig. 3(B) shows a typical spectra obtained by scanning the $\boldsymbol{q}_\parallel$ along the $\Gamma M'$ symmetry direction. The excitation energy of a 2D plasmon is expected to approach 0 as $\boldsymbol{q}_\parallel$ vanishes since the restoring force for a charge density wave in 2D should approach zero at long-wavelength limit. This feature is clearly seen in Fig. 3(B) as expected. Also, quickly increasing linewidth as a function of $\boldsymbol{q}_\parallel$, as can be seen in this figure, is not likely to be explained by single particle excitation.

Long-range dipole field from the plasmon strongly couples with the longitudinal electromagnetic field from slow electrons and scatters them via dipole scattering mechanism [11]. This mechanism yields sharp loss-intensity distribution around the Bragg peaks. In Fig. 4, the intensity of the measured loss is plotted as a function of $\boldsymbol{q}_\parallel$. As we expected, the relative intensity (loss intensity normalized to the (00) spot intensity) is mostly centered around the specular direction, and drops by an order of three with a small wave vector change of 0.15 Å^{-1}. This guarantees that the observed excitation is really dipole active. The dipole lobe is expected to expand to a larger wave vector side as E_p becomes smaller. This effect is actually seen in Fig. 4 when we compare the cases with $E_p = 12.4$ and 5.8 eV. As hallmarked from the above observations, the observed loss is thus identified as a 2D plasma excitation in the surface-state band S1.

The plasmon energy dispersion is plotted as a function of wave vector $\boldsymbol{q}_\parallel$ in Fig. 5. The energy positions of the loss peaks are determined by deconvolution process, using two Lorentzians and a constant background which express the loss peak, the tail from the elastic peak, and the background noise from the pulse-counting system, respectively. The linewidth values were determined by further deconvolution of the loss peaks with respect to the energy and $\boldsymbol{q}$-space resolution of the spectrometer.

In a simplest approximation, based on a classical local response theory, longitudinal plasmon in an infinitely thin film on a semi-infinite dielectric medium is expected to disperse as follows [12].

$$\omega_{2D}(\boldsymbol{q}_\parallel) = [4\pi N_{2D} e^2 m^{*-1} (1 + \varepsilon_{Si})^{-1} \boldsymbol{q}_\parallel]^{1/2} \quad (1)$$

Here, $\omega_{2D}(\boldsymbol{q}_\parallel)$ is the 2D plasma frequency, N_{2D} is the areal density of electrons in the S1 state, $\varepsilon_{Si} = 11.5$ is the dielectric constant of the Si sub-

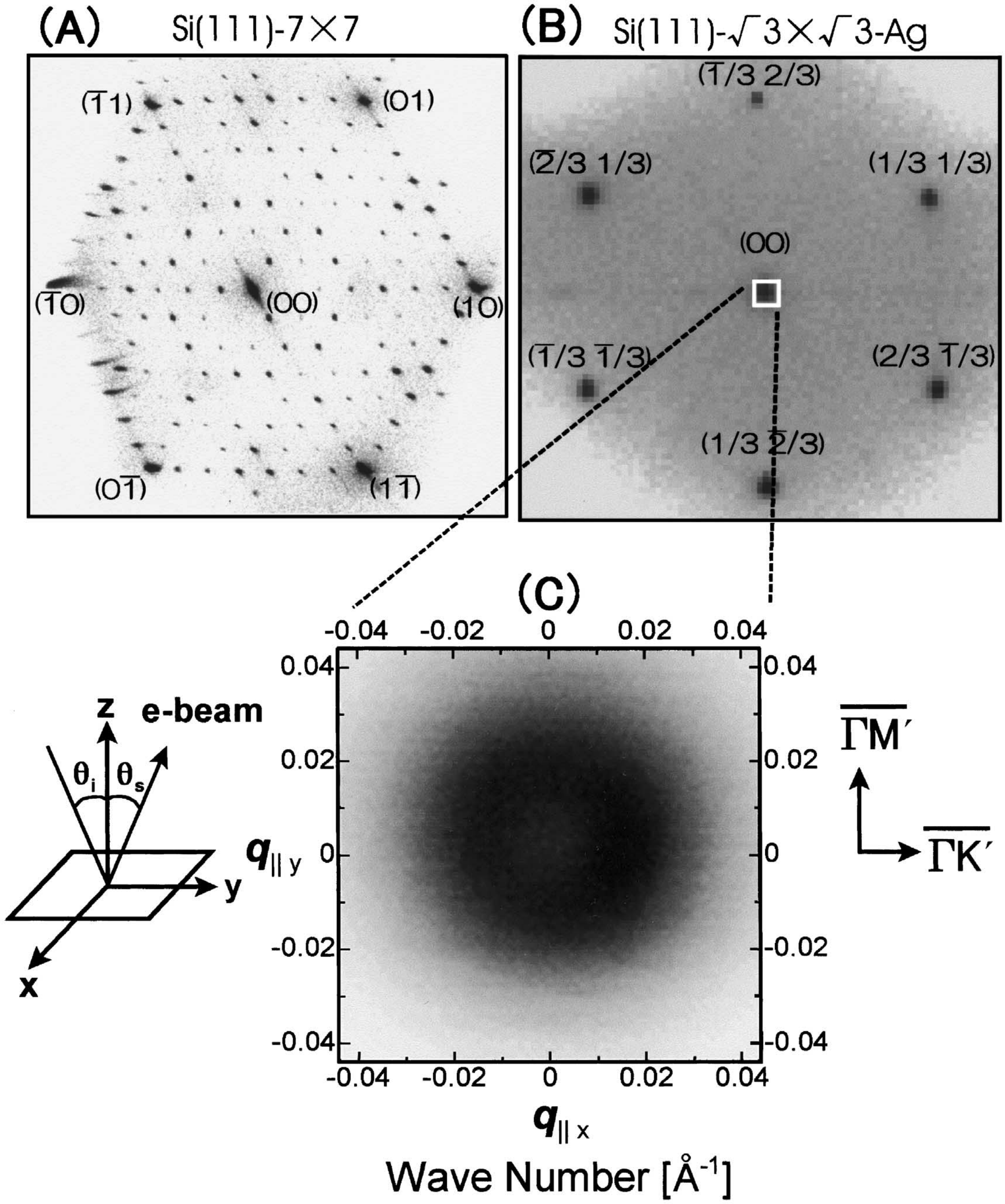

Fig. 2. LEED patterns obtained by ELS-LEED operated in LEED mode. (A) The Clean Si(1 1 1)-7 × 7 surface. (B) The Si(1 1 1)–$\sqrt{3} \times \sqrt{3}$-Ag surface. (C) "Inelastic 2D scan" of the beam scattered from Si(1 1 1)–$\sqrt{3} \times \sqrt{3}$-Ag with an energy loss of 400 meV. Electron primary energy was 50.3 eV for (A) and (B), and 12.3 eV for (C).

strate which is nearly dispersionless within the frequency range of interest [13], m^* is the electron's effective mass, and e is the elementary electric charge.

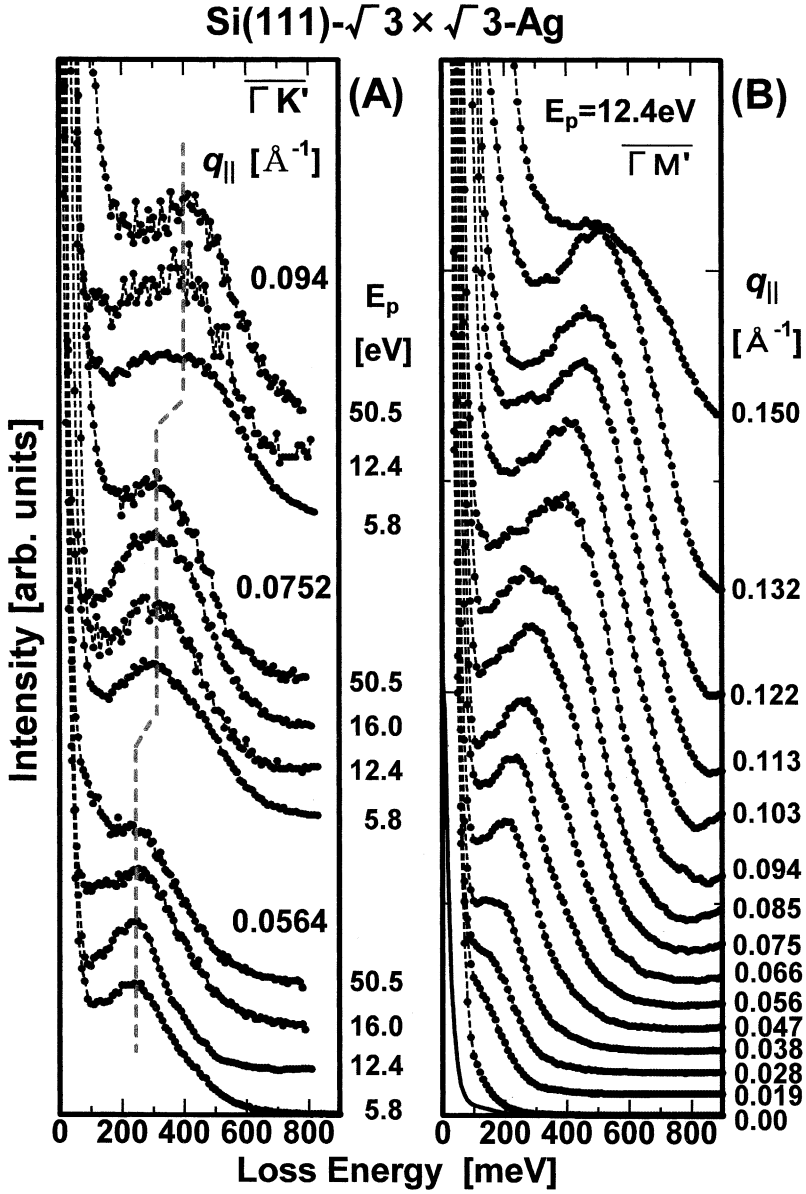

Fig. 3. Angle resolved EELS spectra from the Si(1 1 1)–$\sqrt{3} \times \sqrt{3}$-Ag surface. The energy position of the loss does not change with electron primary energy, but disperses as a function of wave number $\boldsymbol{q}_{\|}$. To ensure the visibility of the loss feature, each spectrum was magnified to compensate for the steep intensity drop by dipole scattering. Also, the spectra obtained at $\boldsymbol{q}_{\|}$ values higher than 0.1 Å^{-1} were smoothed by averaging with 2–5 nearest neighbors.

Our energy dispersion seems to disperse linearly rather than the $\sqrt{\boldsymbol{q}_{\|}}$-type dispersion of Eq. (1). The discrepancy between the $\sqrt{\boldsymbol{q}_{\|}}$ dispersion and the experiment becomes larger as the wave number increases. This is because the local response theory is valid only at small wave number region $\boldsymbol{q}_{\|} \ll k_F$, where k_F is the Fermi wave number of the 2DES.

Within the framework of "nonlocal" response theory using random phase approximation (RPA), Stern has calculated the energy dispersion of a

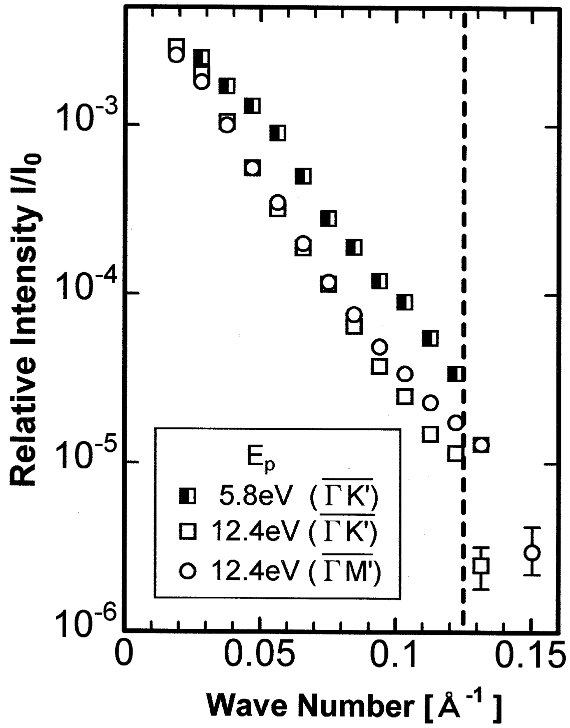

Fig. 4. Relative intensity of the loss peak plotted as a function of wave number $q_{\parallel}$. Vertical dashed line indicates the critical wave number for Landau damping $q_c = 0.125$ Å^{-1} estimated from the RPA calculation shown in Fig. 5.

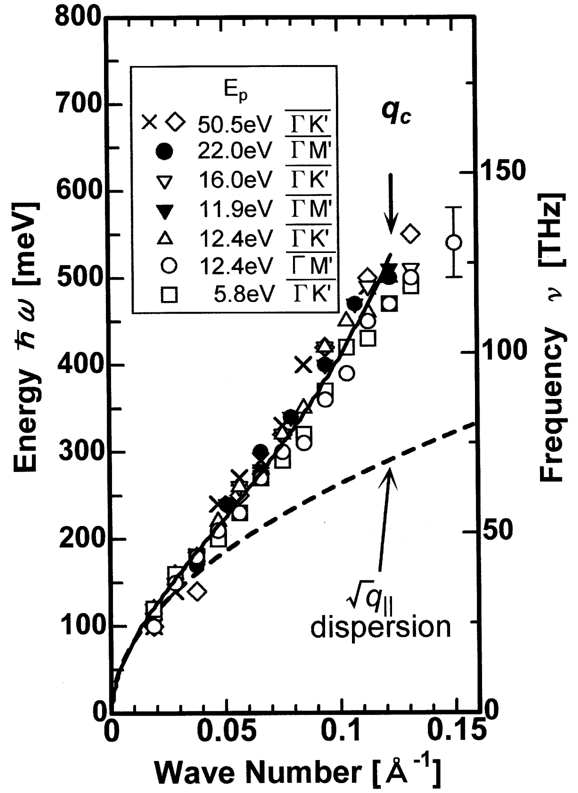

Fig. 5. Plasmon dispersion plot measured with $q_{\parallel}$ scanning along $\Gamma K'$ and $\Gamma M'$ directions. Various electron primary energies E_p ranging from 5.8 to 50.5 eV were used to change the electron probing depth. Filled circle and triangles are the data taken from n-type 15 Ω cm silicon wafer, and the other data are from p-type 0.05 Ω cm wafer. The solid curve is the best fits by full RPA dispersion. For comparison, a $\sqrt{q_{\parallel}}$ dispersion from the local response theory using the same N_{2D} and m^* values are shown by the dashed curve. q_c indicates the onset of Landau damping.

longitudinal plasma in a 2D NFE system [14]. Using this theory, we analyzed the plasmon in a 2DES on a semi-infinite dielectric substrate. For convenience, we show an approximation up to the second-order term in $q_{\parallel}$.

$$\omega_{2D}(q_{\parallel}) = [4\pi N_{2D}e^2 m^{*-1}(1+\varepsilon_{Si})^{-1} q_{\parallel} + 6N_{2D}\hbar^2\pi(2m^*)^{-2} q_{\parallel}^2 + O(q_{\parallel}^3)]^{1/2} \quad (2)$$

The first term is identical to the $\sqrt{q_{\parallel}}$ dispersion from the classical local response theory [12]. The second- and higher-order terms originate from nonlocal effects and reflect the quantum statistics of the 2DES; e.g., the second term is rewritten as $(3/4)v_F^2 q_{\parallel}^2$ with the Fermi velocity v_F of the 2DES and exhibits the degeneracy of the electron system. It should be noted that fitting to the approximated dispersion including only up to the second-order term in Eq. (2) is still not accurate enough compared with the fit to the nonanalytic full RPA dispersion. Although the approximated curve mimics the shape of the experimental curve, the obtained N_{2D} and m^* values are different by several tens of percent from the values determined by the fit to the full RPA curve. This is because the $q_{\parallel}$ range in our experiment is wide enough, ranging up to around k_F, and the effect of higher-order term becomes significant.

The solid curve in Fig. 5 is the best fit to the nonanalytic full RPA dispersion. The overall fit is excellent. The electron density and the electron effective mass are determined to be $N_{2D} = 1.9 \times 10^{13}$ cm^{-2} and $m^* = 0.30m_e$, respectively. Compared with the "local" $\sqrt{\boldsymbol{q}_\parallel}$ dispersion calculated using the same N_{2D} and m^* values (shown by the dashed curve), better agreement between the full RPA dispersion and the experiment at larger $\boldsymbol{q}_\parallel$ region is clearly seen. This indicates the importance of including nonlocal effects and quantum statistics in analyzing the energy dispersion of the 2D plasmons. Moreover, fitting over a wide $\boldsymbol{q}_\parallel$ range with the "nonlocal" full RPA dispersion yields the values of N_{2D} and m^* simultaneously, while in the "local" $\sqrt{\boldsymbol{q}_\parallel}$ case, only their ratio is obtained. The above values of $N_{2D} = 1.9 \times 10^{13}$ cm^{-2} and $m^* = 0.30m_e$ agrees well with the ones obtained from PES measurements, $N_{2D} = (1.6 \pm 0.3) \times 10^{13}$ cm^{-2} and $m^* = (0.29 \pm 0.05)m_e$. Consequently, the estimated Fermi wave number $k_F = (2\pi N_{2D})^{1/2} = 0.109$ Å^{-1} and the Fermi energy of the 2DES, $E_F = 2\pi N_{2D}\hbar^2(2m^*)^{-1} = 0.15$ eV, also agree very well with the reported ones ($k_F = 0.11 \pm 0.01$ Å^{-1}, $E_F = (0.15 \pm 0.1)$ eV [10]).

According to the result of our RPA calculation, the plasmon can exist up to the wave number $\boldsymbol{q}_c = 0.125$ Å^{-1} as shown in Fig. 5 without decaying into electron–hole pairs by strong wave–particle interaction (Landau damping) [1,2]. In the energy-loss spectra, the loss feature also disappears approximately above $\boldsymbol{q}_\parallel = 0.15$ Å^{-1}, accompanied with a significant linewidth broadening as can be seen in the uppermost spectrum in Fig. 3(B). In fact, rapid intensity drop at around $\boldsymbol{q}_\parallel = 0.13$–$0.15$ Å^{-1} is also seen in Fig. 4, and would be assigned to an opening of a new decay channel by Landau damping.

4. Summary

By use of EELS with high-momentum resolution, we have measured the 2D plasma oscillation in a 2DES that consists in a metallic surface-sate band on Si(1 1 1)–$\sqrt{3} \times \sqrt{3}$-Ag. We have found that the energy dispersion is isotropic with respect to the azimuthal orientation and shows no dependence on the electron probing depth. We have clarified that the obtained energy dispersion is well expressed by the 2D RPA theory, and that the estimated electron density and the effective electron mass agree very well with the values reported in PES studies.

Acknowledgements

T.N. acknowledges Profs. T. Inaoka, C. Oshima, A. Liebsch, and H. Ishida for valuable and helpful discussions. He also thanks Drs. V. Zielasek, F. Moresco, E. Hulpke, E. Tamura, A. Nagashima and Prof. J.S. Kim for stimulating discussions. This work has been supported in part by Grants-in-Aid from the Ministry of Education, Science, Culture, and Sports of Japan, especially through the Grants-in-Aid for Creative Basic Scientific Research (no. 08NP1201) conducted by Prof. K. Yagi of Tokyo Institute of Technology.

References

[1] S. Ichimaru, Plasma Physics: An Introduction to Statistical Physics of Charged Particles, Benjamin/Cummings, Menlo Park, CA, 1986 (Chapter 7).
[2] H. Raether, Excitation of Plasmons and Interband Transitions by Electrons, Springer, Berlin, 1980.
[3] P.J. Feibelman, Phys. Rev. Lett. 30 (1973) 975.
[4] W. Plummer, K.-D. Tsuei, B.-O. Kim, Nucl. Instrum. Meth. Phys. Res. B 96 (1995) 448.
[5] M. Rocca, Surf. Sci. Rep. 22 (1995) 1.
[6] A. Liebsch, Electronic Excitations at Metal Surfaces, Plenum Press, New York, 1997.
[7] H. Claus, A. Buessenschuett, M. Henzler, Rev. Sci. Instrum. 63 (1992) 2195.
[8] T. Nagao, S. Hasegawa, Surface and Interface Analysis 30 (2000) 488.
[9] T. Takahashi, S. Nakatani, Surf. Sci. 282 (1993) 17, and references therein.
[10] Y. Nakajima et al., Phys. Rev. B 56 (1997) 6782, and references therein.
[11] H. Ibach, D.L. Mills, Electron Energy Loss Spectroscopy and Surface Vibrations, Academic Press, New York, 1982.
[12] R.H. Ritchie, Phys. Rev. 106 (1957) 874.
[13] H.R. Philipp, H. Ehrenreich, Phys. Rev. 129 (1963) 1550.
[14] F. Stern, Phys. Rev. Lett. 18 (1967) 546.